Multiple-scattering calculations for SiO_2 polymorphs: a comparison to ELNES and XANES spectra

1996 J. Phys.: Condens. Matter 8 3323

(http://iopscience.iop.org/0953-8984/8/19/008)

J. Phys.: Condens. Matter **8** (1996) 3323–3336. Printed in the UK

Multiple-scattering calculations for SiO_2 polymorphs: a comparison to ELNES and XANES spectra

Ziyu Wu†, Friedrich Seifert‡, Brent Poe‡ and Thomas Sharp‡

† Institut de Materiaux de Nantes, CNRS, F-44072 Nantes Cédex 03, France
‡ Bayerisches Geoinstitut, Universität Bayreuth, D-95440 Bayreuth, Germany

Received 14 December 1995, in final form 31 January 1996

Abstract. Experimental XANES and ELNES spectra at the silicon K and $L_{2,3}$ edges and oxygen K edges in three polymorphs of SiO_2 (α-quartz, coesite, and stishovite) are compared to calculated multiple-scattering spectra using different cluster sizes and potentials (X_α and complex Hedin–Lundqvist). The comparison demonstrates that relative energies and intensities of the experimental spectra are well reproduced in the energy range up to $\sim$ 50 eV above the edge by cluster sizes of at least 50 atoms and using the X_α potential. For the tetrahedral structures of α-quartz and coesite further improvement can be obtained by setting the exchange parameter α to 0.828.

1. Introduction

X-ray absorption (XAS) and electron energy loss (EELS) spectroscopy have become in recent years increasingly important tools for structural characterization of materials. In particular the near-edge region (x-ray absorption near-edge structure, XANES, and electron energy loss near-edge structure, ELNES) is able to provide sensitive information on bonding, valence, coordination, etc, where XANES offers the advantage of high energy resolution ($\sim$ 0.05 eV) and ELNES high spatial resolution (down to 0.4 nm).

Although fingerprinting by comparison with structurally known substances is possible (but dangerous in some cases [1] for an empirical interpretation of XANES and ELNES spectra, there has been much recent progress in the calculation of theoretical spectra from first principles (see below), which then also allows more subtle effects to be recognized and explained in the spectra. A requisite for such calculations is, however, that the appropriate form of potential and a sufficient cluster size are employed.

In this paper, we compare the results of multiple-scattering calculations, using different forms of the potentials and different cluster sizes, to experimental (both XANES and ELNES) Si K-edge, Si L-edge, and O K-edge spectra of three polymorphs of SiO_2: the two forms quartz and coesite (based on three-dimensionally connected corner-shared SiO_4 tetrahedra in two different arrangements) and stishovite (rutile structure type, with edge-shared SiO_6 octahedra) in order to find the minimum cluster size that is sufficient (or, vice versa, the length scale that influences the spectra) and the optimum form of potential. This comparison will then form the basis for the later interpretation of chemically and structurally more complex silicates.

0953-8984/96/193323+14$19.50

2. Previous work

High-resolution Si K-edge and L-edge XANES spectra of quartz and stishovite have been reported by Li *et al* [2, 3], and have been compared to theoretical densities of states. Whereas the latter can fairly accurately reproduce the position of most absorption bands, absolute intensities are largely in error. ELNES Si L-, Si K-, and O K-edge spectra for quartz, coesite, and stishovite reported by Sharp *et al* [4] have been compared to preliminary multiple-scattering calculations, using only the X_α potential and moderate cluster sizes. They showed a better agreement of intensities, but in some cases only moderate agreement with respect to the position of absorption bands. Multiple scattering calculations for quartz have recently been summarized by Chaboy *et al* [5]. They demonstrated that fairly large clusters (> 7 Å radius) are needed to reproduce details in the spectra and concluded that a self-consistent field Hedin–Lundqvist (HL) potential is best suited to explain the position and intensities of absorption lines in the Si K-edge spectrum of quartz and amorphous SiO_2, whereas the Si $L_{2,3}$ edge can be reproduced via an X_α potential or the real part of an HL potential. Nevertheless, some disagreements between experimental and calculated spectra persisted.

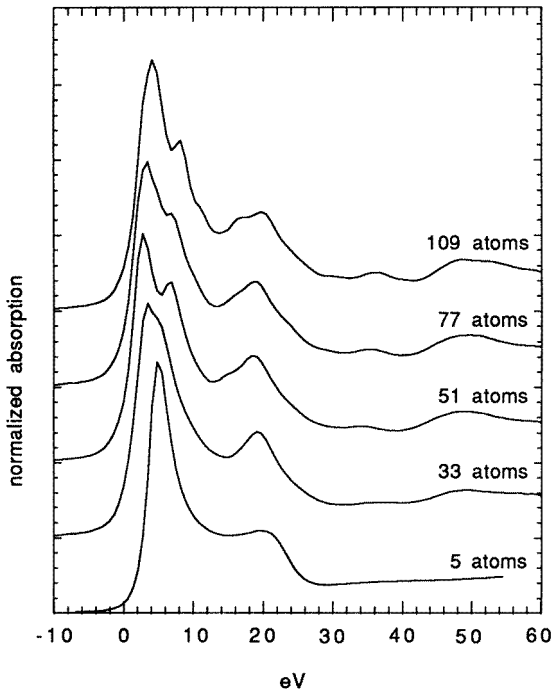

Figure 1. Calculated Si K-edge absortion spectra for quartz as a function of cluster size: X_α potential; convolution with $\Gamma = 1.5$ eV.

Although the structure of vitreous SiO_2 is also based on corner-shared SiO_4 tetrahedra and therefore basically similar to that of quartz, we will not discuss its absorption spectra [6, 7] because its structure is less well constrained than that of crystalline SiO_2 polymorphs.

The following discussion will treat all three most important crystalline SiO_2 polymorphs rather than just quartz. It will be based on new multiple-scattering calculations and the

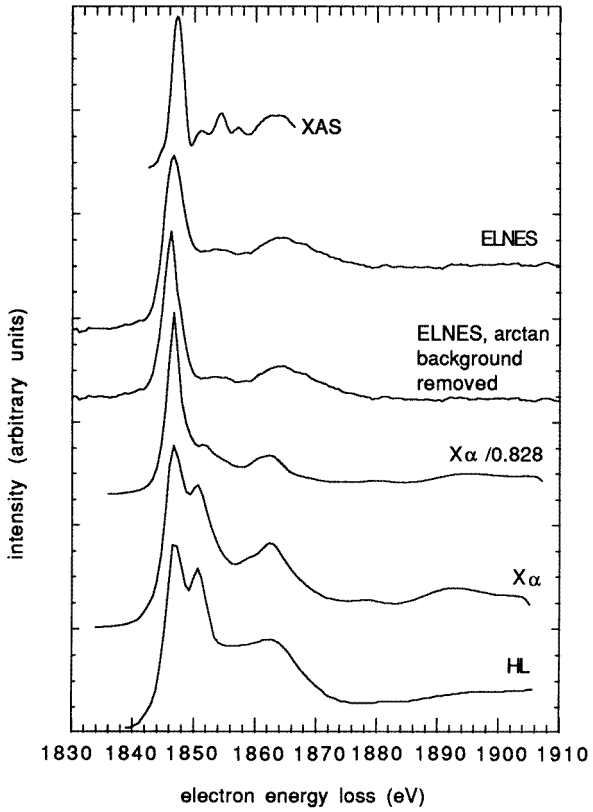

Figure 2. A comparison of experimental XAS [2] and ELNES spectra of the quartz Si K edge to calculated spectra for 51-atom clusters using the HL and X_α potentials.

results will be compared to both published [2–4] x-ray absorption and electron loss data and so-far unpublished ELNES data.

3. Calculation procedures

The XANES/ELNES spectra have been computed using a multiple-scattering approach and programs described elsewhere [4, 8–19]. In the muffin-tin model and one-electron approximation, the local density potential for the system can be constructed on the basis of the Mattheiss prescription [20] by superposition of neutral atomic charge densities using the Clementi–Roetti basis set tables [21]. For the exchange–correlation part of the potential we use two different types: the energy-independent X_α and the energy- and position-dependent complex (HL) self-energy $\Sigma(\boldsymbol{r}, E)$ [22], whose imaginary part gives the amplitude attenuation of the excited photoelectron which is due to inelastic losses and connected to the photoelectron mean free path. Dirac–Hara potential calculations do not show any significant change with respect to the HL results [5]. In the calculations using the X_α potential we have adopted two different values for the exchange parameter α for Si: the one proposed by Schwarz [23] ($\alpha = 0.728$), and a value increased by 0.1 (i.e. $\alpha = 0.828$ cf also Brydson *et al* [24]). The latter calculations are designated as $X_\alpha/0.828$

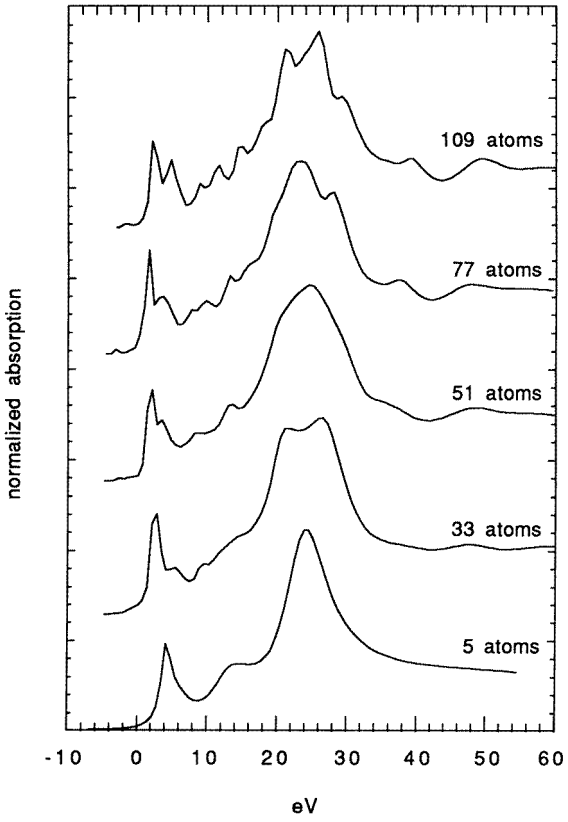

Figure 3. Calculated Si $L_{2,3}$-edge quartz absorption spectra (X_α potential) as a function of cluster size.

in the following.

In order to simulate the charge relaxation around the core hole in the photoabsorber of atomic number Z (14 in the case of Si), we use the well screened $(Z+1)$ approximation (final state rule) [8]. For this the orbitals of the $(Z+1)$ atom are taken and the charge density is constructed by using the excited electronic configuration of the photoabsorber with the core electron promoted to an empty orbital. The consequent solution of the effective Schrödinger equation for the final state is then straightforward. The unpolarized photoabsorption cross section for photons with energy ω, in Rydberg units of energy and lengths, is given by [16]

$$\sigma(\omega) = 2\frac{4\pi^2}{3}\alpha\omega \sum_{L,m_\gamma,m_0} \left| \left\langle \Psi_{kL}^- \left| \left[\frac{4\pi}{3}\right]^{1/2} r Y_{lm_\gamma} \right| \Psi_{L_0} \right\rangle \right|^2 \tag{1}$$

where $\Psi_{kL}^- = (\Psi_{kL}^+)^*$ is the time-reversed scattering wave function in response to an exciting free wave of angular momentum $L = (l, m)$ and Ψ_{L_0} is a core state, usually 1s, 2s, 2p.... The factor of two results from the spin degrees of freedom and $k = \sqrt{E}, E$ being the photoelectron kinetic energy. The calculated spectra are further convoluted with a Lorentzian-shaped function with a full width $\Gamma_h = 0.5$ eV for the Si K edge and ~ 0.02 eV for the L_3 edge [25] to account for the core hole lifetime and $\Gamma_{exp} = 1.0$ eV, the experimental resolution (whereas calculated spectra in [4] are unconvoluted). We have

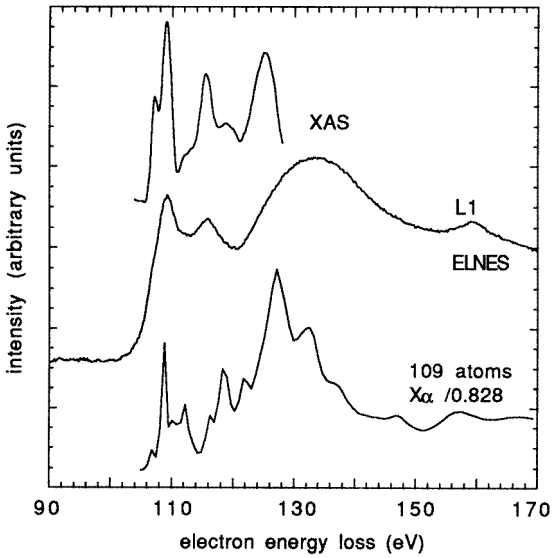

Figure 4. A comparison of experimental XAS [2] and ELNES Si $L_{2,3}$-edge spectra of quartz to a 109-atom cluster multiple-scattering calculation with X_α potential and an exchange parameter of 0.828.

chosen the muffin-tin radii according to the Norman criterion [26] and allowed a 10% overlap between contiguous spheres to simulate the atomic bond.

4. Evaluation of experimental spectra

Whereas the position of absorption bands in XANES spectra is generally well defined due to the high energy resolution, that in ELNES spectra often is not. Therefore, the experimental spectra [4] have been processed in the following way. (i) An exponential background, defined by the pre-edge region, has been subtracted from all spectra. (ii) The Si K-edge spectra have been deconvoluted with the zero-loss peak, which led to a significant improvement of the resolution. Then, a $\tan^{-1}$ function plus Lorentzian lines have been fitted. The number of the latter was confined to that of clearly visible peaks, shoulders, or asymmetries, and no further deconvolution has been attempted. The $\tan^{-1}$-subtracted spectra offer the additional advantage of being directly comparable to the multiple-scattering calculations. However, the parameters of the $\tan^{-1}$ background function are poorly constrained by the spectra [27]. This leads to large uncertainties in the relative intensities of fitted bands, whereas derived peak positions are within ± 0.5 eV for stronger features and generally within ± 1.0 eV for weak features, independent of the precise location of the $\tan^{-1}$ inflection point and the number of lines fitted. (iii) The Si L-edge and O K-edge spectra could not be fitted in this way because the slopes on the low- and high-energy side of the edge are different and thus could not be described by the combination of a single exponential plus $\tan^{-1}$ background [28]. For the Si L edge, an additional complication is the interference of the broad plasmon peak with the pre-edge background. For both Si L-edge and O K-edge spectra we therefore report spectra that are corrected for the exponential background only; positions of bands have been read from these diagrams directly.

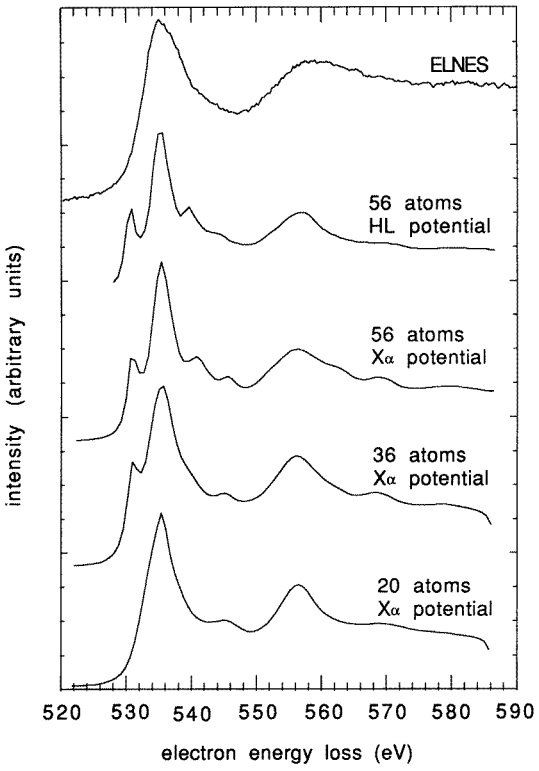

Figure 5. O K-edge ELNES spectrum of quartz compared to calculated spectra using different cluster sizes and potentials (convoluted with 1.0 eV).

5. Results and discussion

Table 1 gives a summary of experimental line positions obtained for the three phases and three edges studied and compares them to published results. In general, agreement between the data of Li *et al* [2] and ours is excellent for the position of major features.

5.1. Quartz

The α-quartz structure consists of an ordered trigonal lattice of interconnected SiO_4 tetrahedra, with two different Si–O distances of 1.5951 and 1.6167 Å. The atomic clusters all have C_2 symmetry relative to the Si site. Atomic coordinates employed for the calculations are those of Zachariasen and Plettinger [29].

In figure 1 we report theoretical spectra based on the X_α potential for the Si K-edge region. The 5–109-atom clusters correspond to spheres of 1.6–7 Å radius around the photoabsorber atom (Si) taken as the centre of the cluster. For comparison with the observed ELNES spectra, we have taken $\Gamma_h = 0.5$ eV and $\Gamma_{exp} = 1.0$ eV. The convoluted total cross sections for clusters correponding to five, 33, 51, 77, and 109 atoms (figure 1) show little change for large (77- and 109-atom) clusters due to the convolution with $\Gamma_{tot} = 1.5$ eV. ELNES and XAS [2] spectra are compared in figure 2 to calculations, all for 51-atom clusters, but with three different potentials: HL complex, X_α, and X_α with the exchange

Table 1. Absorption line positions (eV) in Si K-edge, Si $L_{2,3}$-edge, and O K-edge spectra in quartz, coesite, and stishovite. Uncertainty in absolute line positions of ELNES spectra, ±1.0 eV; energy difference between lines, ±0.5 eV

Quartz		Coesite	Stishovite	
Li *et al* (1993) (XAS)	This study (ELNES)	this study (ELNES)	Li *et al* (1993) (XAS)	This study (ELNES)
Si K edge				
1846.8	1846.7	1846.6	1846.3	
1850.7			1849.0	1848.9
1854.5	1854.5	1856.7	1851.3	
1857.4			1853.4	1852.8
1864.3	1865.2	1866.7	1860.2	
		1892.8	1866.4	1867.0
	1935.6	1932.8		1875.5
				1885.3
				1901.7
				1921.5
Si $L_{2,3}$ edge				
105.43	106.0	106.5	105.95	105.5
106.07			106.75	
107.8	108.4	107.5	109.8	
111.3			113.6	112.5
114.5	115	114	120.7	120
118.5			126.4	126.5
125.0				135
	132	132		140
				150
O K edge				
	535	534		534
	∼542			539
	559	558		555
				564

parameter $\alpha = 0.828$. The spectra based on HL and X_α calculations are identical, except for a slight smoothing beyond 1860 eV due to damping effects in the HL calculations. The best agreement with the ELNES spectrum is achieved by the X_α with $\alpha = 0.828$ potential, not only with respect to relative amplitudes and energies, but also with respect to the width of the white line. Such agreement has not been previously achieved.

The Si $L_{2,3}$ spectra for α-quartz have been computed using the X_α potential and the same atomic clusters, up to about 10 shells (figure 3). The total cross sections without convolution are similar to those of figure 6 in [5]. In the case of the Si $L_{2,3}$ spectra, marked changes still occur at large cluster sizes. However, none of the calculated spectra in figure 3 nor those given by [5] can explain the intensity and position of the band near 120 eV which is a distinct feature in both the XAS and ELNES spectra (cf table 1 and figure 4). Figure 4 presents an improved 109-atom cluster calculation with $\alpha = 0.828$ reproducing all experimental features very well. Also, there is close agreement between our ELNES data (as well as those of Garvie *et al* [30]) and XAS data of Li *et al* [2, 3] in the region up to 122 eV. However, the peak corresponding to the third strong ELNES peak occurs, in XAS, at lower energy and has less intensity. This might be related to the problem of background subtraction in the experimental XAS data as indicated by [5] and [31–33]. Also, figure 3

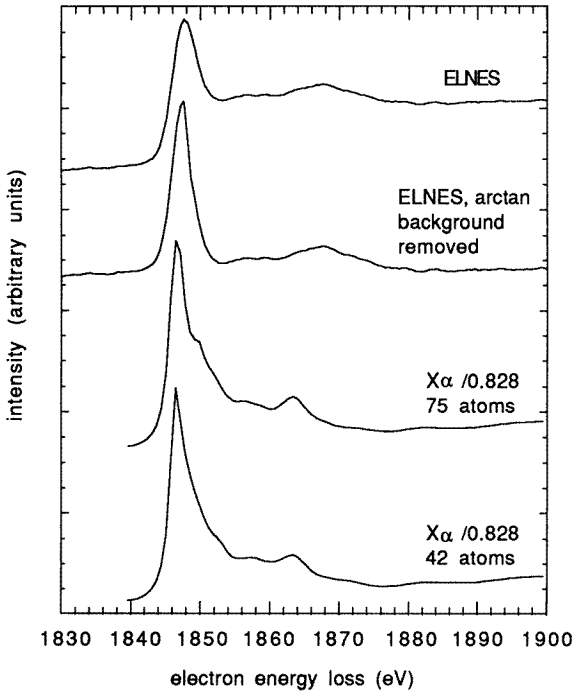

Figure 6. Coesite Si K-edge ELNES spectra compared to calculated spectra using the $X_\alpha/0.828$ potential.

of Li *et al* [3] is in agreement with our spectra.

The model calculations in figure 5 compare the oxygen K-edge ELNES spectra for α-quartz to theoretical spectra for various cluster sizes and the X_α potential and, for comparison, the HL potential. The peaks below and above the main resonance (at 535 eV) appear only when five or more shells are included in the cluster calculations. This behaviour indicates that some lower-energy features are also a result of multiple scattering of the photoelectron within a large cluster, showing that the final state reached in the core electron transition is not a simple atomic or molecular state [34]. Compared to our ELNES experimental spectrum as well as others [35, 36] good agreement is obtained with respect to both relative amplitudes and energies. There is no significant difference between the HL and X_α calculations.

5.2. Coesite

In order to illustrate the behaviour of the tetrahedral Si site in ELNES and XANES experiments, we report similar calculations as for α-quartz for the intermediate-pressure form coesite. It is also based on three-dimensionally connected SiO_4 tetrahedra but with a different framework topology [37]. Si is coordinated by four oxygen atoms with four different Si–O distances (average value, 1.6101 Å). The best agreement between experimental ELNES and theoretical spectra at the Si K edge (figure 6) is obtained, as for α-quartz, with the X_α potential and $\alpha = 0.828$. Increasing the cluster size from 42 to 75 atoms has no significant effect. Coesite exhibits a slightly higher energy separation between the edge

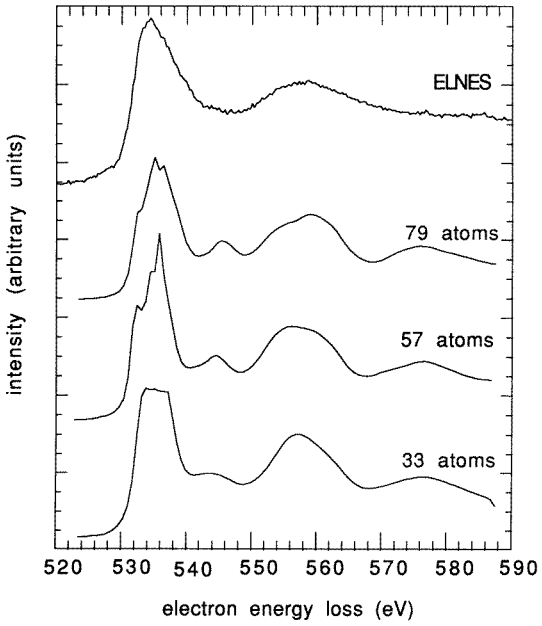

Figure 7. The coesite O K-edge ELNES spectrum compared to multiple-scattering calculations with the X_α potential (convoluted with 1.0 eV).

(1846.6 eV) and the second strong ELNES peak (at 1866.7 eV) than quartz (1846.7 and 1865.2 eV, respectively). The same trend is seen in the MS spectra (X_α potential with $\alpha = 0.828$), where the energy split decreases, for these peaks, from 16.7 eV in coesite to 15.6 eV in quartz. However, the overall similarities of both the experimental spectra and MS calculations to those of quartz confirm the notion of Sharp *et al* [4] that the features are mainly due to short-range structural properties (coordination, bond lengths, and O–Si–O angles).

The Si $L_{2,3}$ calculated spectra and EELS spectra for coesite are very similar to the α-quartz spectra [4] and are not presented here. O K-edge spectra (figure 7) show a close correpondence between the gross features, relative intensity and energy separations, of observed (ELNES) and XANES [35] spectra and those calculated with the X_α potential for various cluster sizes.

5.3. Stishovite

Stishovite, the high-pressure form of SiO_2, has a rutile type structure [38] and is built up by chains of edge-sharing SiO_6 octahedra, with two different Si–O distances, four of 1.7571 Å and two of 1.8082 Å. The symmetry group around the Si photoabsorber is D_{2h}. Atomic coordinates have been taken from the article by Spackman *et al* [39]. Figure 8 gives the Si K-edge spectra calculated with the X_α potential (convoluted with $\Gamma_{tot} = 1.5$ eV) as a function of cluster size up to 105 atoms. An additional calculation for a 153-atom cluster (all atoms within 6.5 Å) shows no further change and thus a good convergence for the 105-atom cluster that correponds to a radius of 5.9 Å. This indicates that the scattering paths of total length greater than about 11.8 Å contribute little to the absorption. The comparison between experimental and calculated spectra (figure 8) shows good correspondence.

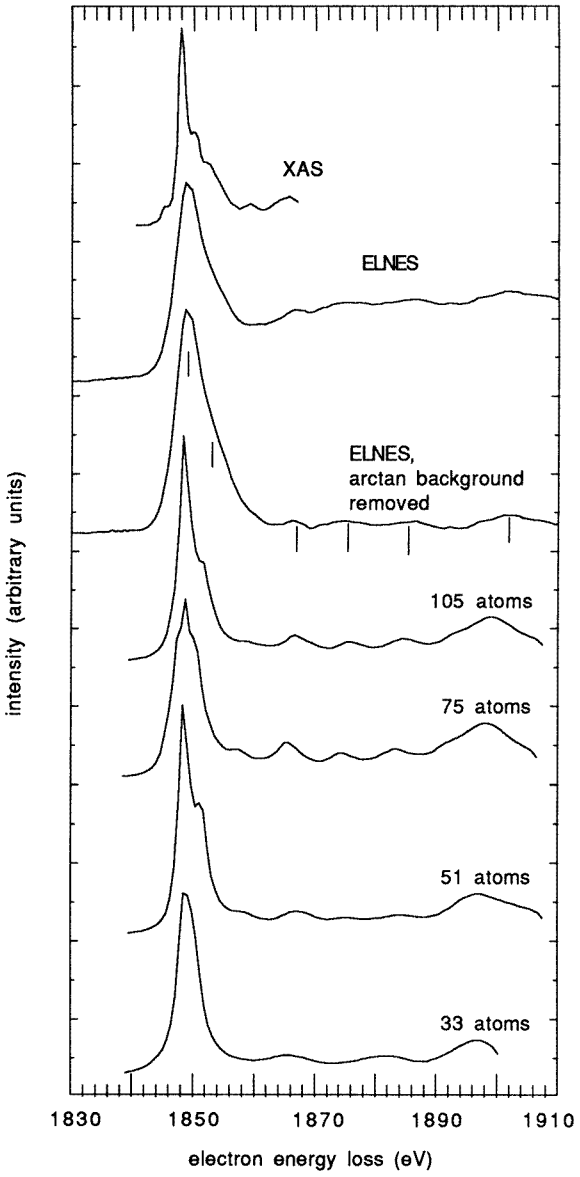

Figure 8. Experimental XAS [2] and ELNES spectra for the Si K edge in stishovite compared to multiple-scattering calculated spectra (X_α potential) as a function of cluster size. Small vertical lines in the ELNES spectrum mark the positions of peaks as found by fitting procedures.

The Si $L_{2,3}$ multiple scattering spectra shown in figure 9 as a function of cluster size and based on the X_α potential (convoluted with $\Gamma_{tot} = 1.0$ eV) demonstrate that the dominant transition features are already present in the seven-atom cluster, i.e. considering only the first oxygen shell around Si. This result can be understood [40, 41] as a caging effect of the oxygen shell on the excited electron: the backscattering creates a relatively sharp quasibound scattering resonance around the absorber atom. As the number of coordination

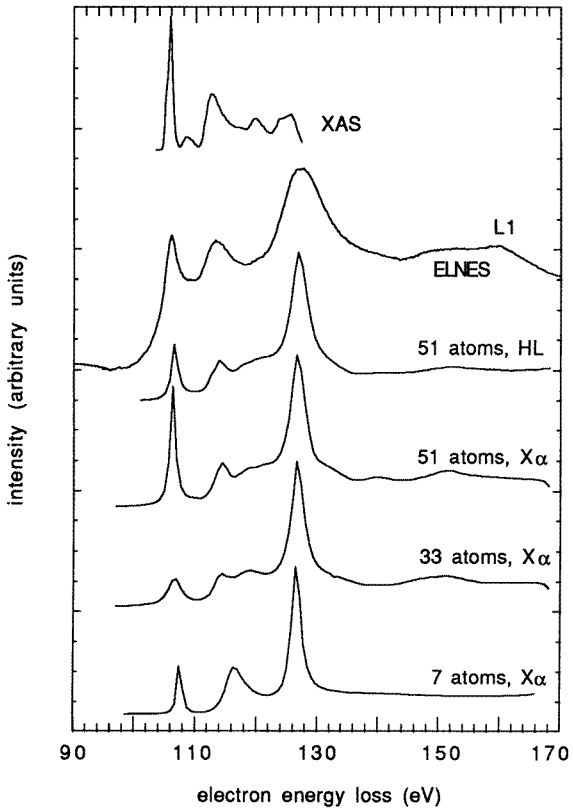

Figure 9. Experimental XAS [2] and ELNES Si $L_{2,3}$ spectra of stishovite compared to multiple-scattering calculated spectra as a function of cluster size and potential. Calculated spectra have been convoluted with $\Gamma = 1.0$ eV. The peak near 160 eV represents the Si L_1 edge which has not been modelled.

shells considered increases, some fine structures are introduced. The comparison between calulations (X_α and HL potentials, which are nearly identical) and observed (ELNES and XANES) spectra in figure 10 exhibits extremely good agreement for not only the fine structure and energies but also the intensities of the different resonances. As for α-quartz we presume that there is a background-subtraction problem for the XAS spectrum at higher energies in the work of Li *et al* [2, 3, 32, 33].

Finally, figure 10 compares the calculated O K-edge spectra for stishovite for two different cluster sizes and two different potentials to the ELNES spectra. The HL potential does not prove to be superior to the X_α potential here either, but rather the X_α calculations for the 61-atom cluster fit the experimental data very well.

6. Conclusions

It has been shown that the gross features of the XAS and ELNES Si K-, Si $L_{2,3}$-, and O K-edge spectra can successfully be modelled with small clusters [4], emphasizing the dominant role of the very first coordination shell. The most striking difference in the spectra and multiple-scattering calculations between SiO_4 and SiO_6 groups is the existence of a strong

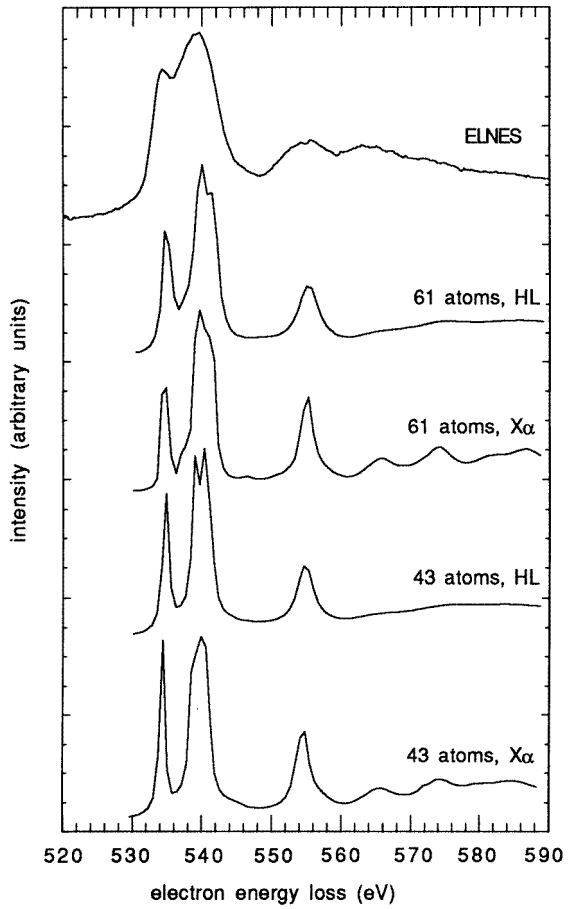

Figure 10. The experimental O K-edge ELNES spectrum in stishovite compared to multiple-scattering calculated spectra.

peak $\sim$ 20 eV above the edge in the Si K-edge spectra of the tetrahedral structures. We explain this by resonance effects between the excited atom and the strong backscatterers (the first oxygen shell). In stishovite, on the other hand, with its SiO_6 groups, the smaller O–Si–O angle reduces the intensity of this peak. These systematic contrasts allow a determination of Si coordination in unknown structures even by the relatively low-resolution ELNES method. Increasing the cluster size, fine structures in the calculations increasingly correspond to those observed in the experimental spectra up to about 50 eV above the edge, pointing to their origin from more distant coordination shells. However, beyond a cluster radius of $\sim$ 7 Å (corresponding to about 100 atoms in silicates) no distinct changes occur in the calculated spectra which leads us to conclude that the maximum length scale of ELNES observation is about 7 Å. This might open the possibility to extract, for unknown structures, information on polyhedral linkage (corner- against edge- against face-sharing polyhedra) in addition to the coordination number in the first shell. We further conclude that the X_α potential is as good as or even superior to the complex Hedin–Lundqvist potential in these SiO_2 polymorphs. For the tetrahedral (α-quartz and coesite) structures, further improvement can be achieved for the Si K and $L_{2,3}$ edges by setting the exchange parameter α to 0.828.

Multiple-scattering theory is thus not only suited for metallic or semiconducting systems but also for insulating materials with partly ionic, partly covalent bonding characteristics.

Acknowledgments

Multianvil synthesis experiments were performed at the Bayerisches Geoinstitut under the EC 'Human Capital and Mobility—Access to Large Scale Facilities' programme (contract No ERBCHGECT940053 to D C Rubie). FS acknowledges support by Fonds der Chemischen Industrie, Frankfurt; BP thanks the Alexander-von-Humboldt Foundation, Bonn, for a fellowship. Helpful discussions with C R Natoli, Frascati, and E Paris, Camerino, are appreciated.

References

[1] McComb D W, Brydson R, Hansen P L and Payne R S 1992 *J. Phys.: Condens. Matter* **4** 8363
[2] Li D, Bancroft G M, Kasrai M, Fleet M E, Feng X H, Tan X H and Yang B X 1993 *Solid State Commun.* **87** 613
[3] Li D, Bancroft G M, Kasrai M, Fleet M E, Secco R A, Feng X H, Tan K H and Yang B X 1994 *Am. Mineral.* **79** 622
[4] Sharp T, Wu Z, Seifert F, Poe B, Doerr M and Paris E *Phys. Chem. Minerals* **23** 17
[5] Chaboy J, Benfatto M and Davoli I 1995 *Phys. Rev.* B **52** 10 014
[6] Davoli I, E Paris, Benfatto M, Fanfoni M, Gargano A, Bianconi A and Seifert F 1992 *Phys. Chem. Minerals* **19** 171
[7] Sutherland D G J, Kasrai M, Bancroft G M, Lui Z F and Tan K H 1993 *Phys. Rev.* B **48** 14 989
[8] Lee P A and Pendry J B 1975 *Phys. Rev.* B **11** 2795
Lee P A and Beni G 1977 *Phys. Rev.* B **15** 2862
[9] Natoli C R, Misemer D K, Doniach S and Kutzler F W 1980 *Phys. Rev.* A **22** 1104
[10] Durham P J, Pendry J B and Hodges C H 1982 *Comput. Phys. Commun.* **25** 193
[11] Natoli C R and Benfatto M 1986 *J. Physique Coll.* **47** C8 11
[12] Natoli C R, Benfatto M and Doniach S 1986 *Phys. Rev.* B **34** 4682
[13] Durham P J 1988 *Chemical Analysis* vol 92, ed D C Konigsberger and R Prins (New York: Wiley) p 72
[14] Natoli C R, Benfatto M, Brouder C, Ruiz Lopez M Z and Foulis D L 1990 *Phys. Rev.* B **42** 1944
[15] Rehr J J, Mustre de Leon J, Zabinsky S I and Albers R C 1991 *J. Am. Chem. Soc.* **113** 5315
[16] Tyson T A, Hodgson K O, Natoli C R and Benfatto M 1992 *Phys. Rev.* B **46** 5997
[17] Wu Z Y, Benfatto M and Natoli C R 1992 *Phys. Rev.* B **45** 531; 1993 *Solid State Commun.* **87** 475
[18] Wu Z Y, Mottana A, Marcelli A and Paris E *Phys. Chem. Minerals* at press
[19] Paris E, Wu Z Y, Mottana A and Marcelli A *Eur. J. Mineral* at press
[20] Mattheiss L 1964 *Phys. Rev.* A **13** 970
[21] Clementi E and Roetti C 1974 *At. Data Nucl. Data Tables* **14**
[22] Chou H, Rehr J J, Stern E A and Davidson E R 1987 *Phys. Rev.* B **35** 2604 and references therein
[23] Schwarz K 1972 *Phys. Rev.* B **5** 2466
[24] Brydson R, Sauer H, Engel W, Thomas J M, Zeitler E, Kosugi N and Kuroda H 1989 *J. Phys.: Condens. Matter* **1** 797
[25] Fuggle J C and Inglesfield J E 1992 *Unoccupied Electronic States, Topics in Applied Physics* (Berlin: Springer) appendix B, p 347
[26] Norman G 1974 *Mol. Phys.* **81** 1191
[27] Boland J J, Halaka F G and Baldeschwieler J D 1983 *Phys. Rev.* B **28** 2921
[28] Wilson A R 1991 *Microsc. Microanal. Microstruct.* **2** 269
[29] Zachariasen W H and Plettinger H A 1965 *Acta Crystallogr.* **18** 710
[30] Garvie L A J, Craven A J and Brydson R 1994 *Am. Mineral* **79** 411
[31] Bianconi A 1979 *Surf. Sci.* **89** 41
[32] Hansen P L, Brydson R and McComb D M 1992 *Microsc. Microanal. Microstruct.* **3** 213
Harp G R, Saldini D K and Tonnert B P 1993 *J. Phys.: Condens. Matter* **5** 5377
[33] Brytov I A, Konashenok K I and Romashchenko Yu N 1979 *Geochem. Int.* **16** 142

[34] Soldatov A V, Ivanchenko T S, Della Longa S, Kotani A, Iwamoto Y and Bianconi A 1994 *Phys. Rev.* B **50** 5074
[35] Brown G E Jr, Waychunas G A, Stohr J and Sette F 1986 *J. Physique Coll.* **47** C8 12 685
[36] Bart F, Jollet F, Duirand J P and Douillard L 1993 *Phys. Status Solidi* b **176** 163
[37] Geisinger K L, Spackman M A and Gibbs G V 1987 *J. Phys. Chem.* **91** 3237
[38] Hill R J, Newton M D and Gibbs G V 1983 *J. Solid State Chem.* **47** 185
[39] Spackman M A, Hill R J, Gibbs G V 1987 *Phys. Chem. Minerals* **14** 139
[40] Vvedensky D D and Pendry J B 1985 *Phys. Rev. Lett.* **54** 2725
[41] Lindner Th, Sauer H, Engel W and Kamber K 1986 *Phys. Rev.* B **33** 22